

## Comparative Study of Structure–Properties Relationship for Novel $\beta$ -Halogenated Lanthanide Porphyrins and Their Nickel and Free Bases Precursors, as a Function of Number and Nature of Halogens Atoms<sup>‡</sup>

G. A. Spyroulias,<sup>†‡</sup> A. P. Despotopoulos,<sup>†</sup> C. P. Raptopoulou,<sup>§</sup> A. Terzis,<sup>§</sup> D. de Montauzon,<sup>||</sup> R. Poilblanc,<sup>||</sup> and A. G. Coutsolelos<sup>\*†</sup>

Department of Chemistry, Laboratory of Bioinorganic Coordination Chemistry, School of Science, University of Crete, P.O. Box 1470, 714 09, Heraklion, Crete, Greece, Institute of Materials Science, NCRS “Demokritos”, 15310 Agia Paraskevi, Athens, Greece, and Laboratoire de Chimie de Coordination, CNRS, UPR 8241 liée par convention à l’Université Paul Sabatier et à l’Institut Polytechnique de Toulouse, 205 route de Narbonne, 31077-Toulouse Cedex, France

Received July 5, 2000

The synthetic route of partially  $\beta$ -halogenated via a “metal-assisted” reaction and perhalogenated terbium complexes is described. This protocol allows the facile insertion of the halogens (bromines or chlorides) to the porphyrin peripheral positions. The electronic absorption spectra and the redox potentials of the free porphyrins as well as the terbium complexes are dramatically affected as the number of halogen atoms increase. In fact, two antagonistic effects are responsible for that, the inductive and the distortion effects on the porphyrin ring. They result in a red shift for the Soret band and a stabilization/destabilization of the HOMOs/LUMOs which in turn is manifested by variations on the redox potentials. The novel crystal structure of the Ni(Cl<sub>8</sub>TPP) is discussed in great detail and compared with the previously reported structures of Tb(Cl<sub>8</sub>TPP) (OAc)(DMSO)<sub>2</sub>·3PhCH<sub>3</sub>·MeOH and H<sub>2</sub>(Br<sub>8</sub>TPP), as well as with other perhalogenated nickel porphyrins available in the literature.

### Introduction

The first report of the *meso*-tetrakis-(2,6-dichloro-phenyl)-porphyrin<sup>1</sup> was followed by an increased development of new synthetic routes toward the halogenation of the porphyrin ring as effective and robust catalysts.<sup>2–4</sup>

Although  $\beta$ -substituted, mainly halogenated, porphyrins had appeared by the mid-1970s,<sup>5–7</sup> it was almost 10 years

later when they were successfully used for olefin epoxidation and alkane hydroxylation reactions and were established as remarkably active and robust catalysts.<sup>8–16</sup> In  $\beta$ -halogenated porphyrins possessing more than four halogens in the pyrrole positions, nitrogen basicity is considerably decreased because of the electron-withdrawing effect of the peripheral substituents to the macrocycle. Introduction of halogens to the  $\beta$ -pyrrole carbons results in the distortion of the macrocycle,

<sup>‡</sup> This contribution is dedicated to the memory of our colleague and friend, Dominique de Montauzon.

\* To whom correspondence should be addressed. E-mail: coutsole@chemistry.ucl.ac.uk. Phone: ++30.810.393636. Fax: ++30.810.393601 or ++30.810.393671 PCmodem.

<sup>†</sup> University of Crete.

<sup>‡</sup> Current address: Center of Magnetic Resonance—CERM, Department of Chemistry, University of Florence, Polo Scientifico, Via L. Sacconi 6, IT-50019 Sesto Fiorentino (FI), Italy.

<sup>§</sup> Institute of Materials Science, NCRS “Demokritos”.

<sup>||</sup> L’Université Paul Sabatier et à l’Institut Polytechnique de Toulouse.

- (1) Traylor, P. S.; Dolphin, D.; Traylor, T. G. *J. Chem. Soc., Chem. Commun.* **1984**, 279.
- (2) Grinstaff, M. W.; Hill, M. G.; Labinger, J. A.; Gray, H. B. *Science* **1994**, *264*, 1311.
- (3) Dolphin, D.; Traylor, T. G.; Xie, L. Y. *Acc. Chem. Res.* **1997**, *30*, 251.
- (4) Lyons, J. E.; Ellis, P. E. *Metalloporphyrins in Catalytic Oxidations*; Dekker: New York, 1994; p 297.
- (5) Callot, H. J. *Tetrahedron Lett.* **1973**, *50*, 4987.

- (6) Callot, H. J. *Bull. Soc. Chim. Fr.* **1974**, 7–8, 1492.
- (7) Giraudeau, A.; Callot, H. J.; Jordan, J.; Ezhar, I.; Gross, M. *J. Am. Chem. Soc.* **1979**, *101*, 3857.
- (8) Traylor, T. G.; Tsuchiya, S. *Inorg. Chem.* **1987**, *26*, 1338.
- (9) Carrier, M.-N.; Scheer, C.; Gouvine, P.; Bartoli, J.-F.; Battioni, P.; Mansuy, D. *Tetrahedron Lett.* **1990**, *31*, 6645.
- (10) Battioni, P.; Brigaud, O.; Desvaux, H.; Mansuy, D.; Traylor, T. G. *Tetrahedron Lett.* **1991**, *32*, 2893.
- (11) Bartoli, J.-F.; Brigaud, O.; Battioni, P.; Mansuy, D. *J. Chem. Soc., Chem. Commun.* **1991**, 440.
- (12) Campestrini, S.; Meunier, B. *Inorg. Chem.* **1992**, *31*, 1999.
- (13) Meunier, B. *Chem. Rev.* **1992**, *92*, 1411. Collman, J. P.; Zhang, X.; Lee, V. J.; Uffelman, E. S.; Brauman, J. I. *Science* **1993**, *261*, 1404.
- (14) Mansuy, D. In *The Activation of Dioxigen and Homogeneous Catalytic Oxidation*; Barton, D. H. R., Martell, A. E., Eds.; Plenum: New York, 1993; p 347.
- (15) Collman, J. P.; Zhang, X.; Lee, V. J.; Uffelman, E. S.; Brauman, J. I. *Science* **1993**, *261*, 1404.
- (16) Mansuy, D. *Coord. Chem. Rev.* **1993**, *125*, 129.

and this effect is pronounced when more than four halogens replace the corresponding pyrrole hydrogens. Consequently, a red shift of the Soret band transition energy and a decrease in the HOMO–LUMO energy gap expressed via the large shift of the redox potentials of the porphyrin ring have been observed.<sup>17–29</sup> The  $\beta$ -halogenated porphyrin derivatives with iron or manganese are considered as mimetic models for cytochrome P450s because of their similar catalytic activity. Also, such perhalogenated derivatives have been studied in suprabiotic catalysis<sup>30,31</sup> while only recently D. Dolphin communicated that the iron  $\beta$ -halogenated derivative of 5,10,15,20-tetrakis(2,6-dichlorophenyl)-porphyrin oxidizes the analgesic lidocaine in a similar way to that of mammalian livers.<sup>32</sup>

Although there are recent advances in the development of the  $\beta$ -halogenated<sup>33–38</sup> or other symmetrical or unsymmetrical  $\beta$ -substituted porphyrins,<sup>39–47</sup> as well as the ultimately synthesized perfluorinated<sup>48,49</sup> or pernitrate<sup>50,51</sup> porphyrins, the development of new improved, simplified

protocols for high yield,  $\beta$ -tetra- or octahalogenated porphyrins still remains a major challenge.

Metalation of porphyrins with lanthanides results in two different classes of interesting complexes: the lanthanide monoporphyrinates and the lanthanide “sandwich-like” bisporphyrinates. The former compounds were reported in the early 1970s<sup>52,53</sup> and studied as photochemical probes,<sup>54–56</sup> NMR shift reagents,<sup>57,58</sup> and contrast agents,<sup>59</sup> while the latter species appeared almost 10 years later<sup>60,61</sup> and have been extensively studied as models of the active center, the so-called “special pair”, in the photosynthetic bacteria.<sup>62–66</sup> The axial ligation of the Ln metal center, for the Ln monoporphyrinates, was debated for a long time.<sup>67</sup> Only recently has the first X-ray crystal structure determination of a lanthanide monoporphyrinate been reported by our group,<sup>29</sup> several years after the crystal structure of the acetatolutetium monophthalocyaninate, [Lu(OAc)(Pc)(H<sub>2</sub>O)<sub>2</sub>]·H<sub>2</sub>O·2MeOH.<sup>68</sup>

We report here the detailed synthetic procedures for the synthesis of  $\beta$ -tetra- or octachlorinated and the corresponding brominated 5,10,15,20-tetraphenylporphyrin derivatives, the structural, optical and electrochemical properties of the parent Ni halogenated porphyrins, their demetalation products (free bases), and the corresponding Tb monoporphyrinic complexes.

## Experimental Section

**General Information.** Dichloromethane, CH<sub>2</sub>Cl<sub>2</sub>, and 1,2,4-trichlorobenzene, 1,2,4-tcb, were purchased from Riedel-de Haen and

- (17) Wijesekera, T.; Matsumoto, A.; Dolphin, D.; Lexa, D. *Angew. Chem., Int. Ed. Engl.* **1990**, *29*, 1028.
- (18) Ochsenbein, P.; Mandon, D.; Fischer, J.; Weiss, R.; Austin, R. N.; Jayaraj, K.; Gold, A.; Terner, J.; Bill, E.; Muther, M.; Trautwein, A. X. *Angew. Chem., Int. Ed. Engl.* **1993**, *32*, 1437.
- (19) Mandon, D.; Ochsenbein, P.; Fischer, J.; Weiss, R.; Jayaraj, K.; Austin, R. N.; Gold, A.; White, P. S.; Brigaud, O.; Battioni, P.; Mansuy, D. *Inorg. Chem.* **1992**, *31*, 2044.
- (20) Brigaud, O.; Battioni, P.; Mansuy, D.; Giessner-Prettre, C. *Nouv. J. Chim.* **1992**, *16*, 1031.
- (21) Takeuchi, T.; Gray, H. B.; Goddard, W. A., III. *J. Am. Chem. Soc.* **1994**, *116*, 9730.
- (22) Hodge, J. A.; Hill, M. G.; Gray, H. B. *Inorg. Chem.* **1995**, *34*, 809.
- (23) Brinbaum, E. R.; Schaefer, W. P.; Labinger, J. A.; Bercaw, J. E.; Gray, H. B. *Inorg. Chem.* **1995**, *34*, 1751.
- (24) Brinbaum, E. R.; Hodge, J. A.; Grinstaff, M. W.; Schaefer, W. P.; Henling, L.; Labinger, J. A.; Bercaw, J. E.; Gray, H. B. *Inorg. Chem.* **1995**, *34*, 3625.
- (25) Grinstaff, M. W.; Hill, M. G.; Brinbaum, E. R.; Schaefer, W.; Labinger, J. A.; Gray, H. B. *Inorg. Chem.* **1995**, *34*, 4896.
- (26) Kadish, K.; D’Souza, F.; Villard, A.; Autret, M.; Van Caemelbecke, E.; Bianco, P.; Antonini, A.; Tagliatesta, P. *Inorg. Chem.* **1994**, *33*, 5169.
- (27) Tagliatesta, P.; Li, J.; Autret, M.; Van Caemelbecke, E.; Villard, A.; D’Souza, F.; Kadish, K. *Inorg. Chem.* **1996**, *35*, 5570.
- (28) Autret, M.; Ou, Z.; Antonini, A.; Boschi, T.; Tagliatesta, P.; Kadish, K. *J. Chem. Soc., Dalton Trans.* **1996**, 2793.
- (29) Spyroulias, G. A.; Despotopoulos, A.; Raptopoulou, C. P.; Terzis, A.; Coutsolelos, A. G. *J. Chem. Soc., Chem. Commun.* **1997**, 783.
- (30) Ellis, P. E., Jr.; Lyons, J. E. *Catal. Lett.* **1989**, *3*, 389.
- (31) Lyons, J. E.; Ellis, P. E., Jr. *Catal. Lett.* **1991**, *8*, 45.
- (32) Chorghade, M. S.; Hill, D. R.; Lee, E. C.; Pariza, R. J.; Dolphin, D.; Hino, F.; Zhang, L.-Y. *Pure Appl. Chem.* **1996**, *68*, 753.
- (33) Bhyrappa, P.; Krishnan, V. *Inorg. Chem.* **1991**, *30*, 239.
- (34) Bhyrappa, P.; Krishnan, V.; Nethaji, M. *J. Chem. Soc., Dalton Trans.* **1993**, 1901.
- (35) Hoffmann, P.; Robert, A.; Meunier, B. *Bull. Soc. Chim. Fr.* **1992**, *129*, 85.
- (36) For a recent study on conformational properties of some newly synthesized  $\beta$ -substituted porphyrins see: Nurco, D. J.; Medforth, C. J.; Forsyth, T. P.; Olmstead, M. M.; Smith, K. M. *J. Am. Chem. Soc.* **1996**, *118*, 10918.
- (37) Wijesekera, T.; Dupre, D.; Cader, M. S. R.; Dolphin, D. *Bull. Soc. Chim. Fr.* **1996**, *133*, 765.
- (38) Chorghade, M. S.; Dolphin, D.; Dupre, D.; Hill, D. R.; Lee, E. C.; Wijesekera, T. P. *Synthesis* **1996**, 1320.
- (39) Medforth, C. J.; Smith, K. M. *Tetrahedron Lett.* **1990**, *31*, 5583.
- (40) Takeda, J.; Ohya, T.; Sato, M. *Chem. Phys. Lett.* **1991**, *188*, 384.
- (41) Tsuchiya, S. *J. Chem. Soc., Chem. Commun.* **1991**, 716.
- (42) Takeda, J.; Sato, M. *Tetrahedron Lett.* **1994**, *35*, 3565.
- (43) Chan, K. S.; Zhou, X.; Luo, B.-S.; Mak, T. C. W. *J. Chem. Soc., Chem. Commun.* **1994**, 271.
- (44) Zhou, X.; Zhou, Z.-Y.; Mak, T. C. W.; Chan, K. S. *J. Chem. Soc., Perkin Trans. 1* **1994**, 2519.
- (45) Atkinson, S. T.; Brady, S. P.; James, J. P.; Nolan, K. B. *Pure Appl. Chem.* **1995**, *67*, 1109.
- (46) Zhou, X.; Tse, M. K.; Wan, T. S. M.; Chan, K. S. *J. Org. Chem.* **1996**, *61*, 3590.
- (47) Ricciardi, G.; Bavoso, A.; Bencini, A.; Rosa, A.; Lelj, F.; Bonosi, F. *J. Chem. Soc., Dalton Trans.* **1996**, 2799.
- (48) Woller, E. K.; DiMugno, S. G. *J. Org. Chem.* **1997**, *62*, 1588.
- (49) Leroy, J.; Bondon, A.; Toupet, L.; Rolando, C. *Chem. Eur. J.* **1997**, *3*, 1890.
- (50) Bartoli, J.-F.; Battioni, P.; De Foor, W. R.; Mansuy, D. *J. Chem. Soc., Chem. Commun.* **1994**, 23.
- (51) Ozette, K.; Leduc, P.; Palacio, M.; Bartoli, J.-F.; Barkigia, K. M.; Fajer, J.; Battioni, P.; Mansuy, D. *J. Am. Chem. Soc.* **1997**, *119*, 6442.
- (52) Wong, C.-P.; Venteicher, R. F.; Horrocks, D. W., Jr. *J. Am. Chem. Soc.* **1974**, *96*, 7149.
- (53) Wong, C.-P.; Horrocks, D. W., Jr. *Tetrahedron Lett.* **1975**, 2637.
- (54) Horrocks, D. W., Jr.; Venteicher, R. F.; Spilburg, C. A.; Vallee, B. L. *Biochem. Biophys. Res. Commun.* **1975**, *64*, 317.
- (55) Gouterman, M.; Schumaker, B. D.; Srivastava, T. S.; Yotenani, T. *Chem. Phys. Lett.* **1976**, *40*, 456.
- (56) Horrocks, D. W., Jr.; Goncalves J. *Phys. Chem.* **1976**, *80*, 2389.
- (57) Horrocks, D. W., Jr.; Wong, C.-P. *J. Am. Chem. Soc.* **1976**, *98*, 7157.
- (58) Horrocks, D. W., Jr.; Hove, E. G. *J. Am. Chem. Soc.* **1978**, *100*, 4386.
- (59) Lauffer, R. B. *Chem. Rev.* **1987**, *87*, 901.
- (60) Buchler, J. W.; Kapellmann, H. G.; Knoff, M.; Lay, K.-L.; Pfeifer, S. *Z. Naturforsch.* **1983**, *38b*, 1339.
- (61) Buchler, J. W.; Elsasser, K.; Kihn-Botulinski, M.; Scharbert, B. *Angew. Chem., Int. Ed. Engl.* **1986**, *25*, 286.
- (62) Buchler, J. W.; De Cian, A.; Fischer, J.; Hammerschmitt, P.; Loffler, J.; Scharbert, B.; Weiss, R. *Chem. Ber.* **1989**, *122*, 2219.
- (63) Spyroulias, G. A.; Coutsolelos, A. G.; Raptopoulou, C. P.; Terzis, A. *Inorg. Chem.* **1995**, *34*, 2476.
- (64) Chabach, D.; Tahiri, M.; De Cian, A.; Fischer, J.; Weiss, R.; El Maloul Bibout, M. *J. Am. Chem. Soc.* **1995**, *117*, 8548.
- (65) Kadish, K. M.; Moninot, G.; Hu, Y.; Dubois, D.; Ibnlfassi, A.; Barbe, J.-M.; Guillard, R. *J. Am. Chem. Soc.* **1993**, *115*, 8153.
- (66) Girolami, G. S.; Hein, C. L.; Suslick, K. S. *Angew. Chem., Int. Ed. Engl.* **1996**, *35*, 1223.
- (67) Buchler, J. W.; Kihn-Botulinski, M.; Loffler, J.; Scharbert, B. *New J. Chem.* **1992**, *16*, 545.
- (68) De Cian, A.; Moussavi, M.; Fischer, J.; Weiss, R. *Inorg. Chem.* **1985**, *24*, 3162.

Aldrich, respectively, and used as received. Tetrahydrofuran, THF, was purchased from Merck and distilled under argon and over a mixture of sodium/benzophenone. Tetra-*n*-butylammonium perchlorate, TBAP, purchased from Fluka, was recrystallized from absolute ethanol and then dried in a vacuum oven at 40 °C. *N*-Bromo- and chlorosuccinimide were purchased from Fluka and were either purified as reported in the literature<sup>69</sup> or used as received. All synthetic procedures were performed under an argon stream.

**Instrumentation and Methods.** Absorption spectra were collected on a Perkin-Elmer Lambda 6 grating spectrophotometer. Spectra for  $\epsilon$  measurements were recorded in CH<sub>2</sub>Cl<sub>2</sub> or PhCH<sub>3</sub> (solutions of  $0.05 \times 10^{-3}$  M). Electrochemistry experiments carried out with a homemade potentiostat using interfacing hardware with a PC-compatible microcomputer. The positive feedback (scan rate  $> 1 \text{ V}\cdot\text{s}^{-1}$ ) or interrupt (scan rate  $< 1 \text{ V}\cdot\text{s}^{-1}$ ) methods were used to compensate for uncompensated resistance (IR) drop. Electrochemical experiments were performed in an airtight three-electrode cell connected to a vacuum/argon line. The cell was degassed and filled according to standard vacuum techniques. The reference electrode consisted of a saturated calomel electrode (SCE) separated from the solution by a bridge-compartment filled with a solution of the same supporting electrolyte in the same solvent as that used in the cell. The counter-electrode was a spiral of  $\sim 1 \text{ cm}^2$  apparent surface area, made of a 8 cm-long and 0.5 mm-diameter platinum wire. The working electrode was a rotating disk electrode (RDE) with a 2 mm-diameter Pt disk (Tacussel EDI) or an ultramicroelectrode consisting of a 100  $\mu\text{m}$ -diameter Pt disk.

**Porphyryns.** H<sub>2</sub>(TPP) and Ni(TPP) were synthesized, according to literature procedures [abbreviations: (OEP)<sup>2-</sup> = 2,3,7,8,12,13,17,18-octaethyl porphyrinate; (TPP)<sup>2-</sup> = 5,10,15,20-tetraphenyl porphyrinate; [Cl<sub>8</sub>TPP]<sup>2-</sup> = 2,3,7,8,12,13,17,18-octa- $\beta$ -chloro-5,10,15,20-tetrakis(phenyl) porphyrinate; [Br<sub>8</sub>TPP]<sup>2-</sup> = 2,3,7,8,12,13,17,18-octa- $\beta$ -bromo-5,10,15,20-tetrakis(phenyl) porphyrinate; [Cl<sub>4</sub>TPP]<sup>2-</sup> = tetra- $\beta$ -chloro-5,10,15,20-tetrakis(phenyl); and [Br<sub>4</sub>TPP]<sup>2-</sup> = tetra- $\beta$ -bromo-5,10,15,20-tetrakis(phenyl) porphyrinate dianions].<sup>70</sup> The synthetic procedures described for all the tetra- and octahalogenated porphyryns are modified protocols reported only on the synthesis of octachloroporphyrin.<sup>17</sup>

**$\beta$ -Tetrachloro-5,10,15,20-tetraphenylporphinato Nickel, 1.** To a solution of 1.0 g (1.50 mmol) of Ni(TPP) in 60 mL of 1,2-*o*-dichlorobenzene was added 800 mg (6.0 mmol) of *N*-chlorosuccinimide. The solution was brought to reflux for 2 h. The reaction was monitored by UV-vis spectroscopy (the Soret band shifted from 411 to 425 nm). After the end of the reaction, the solvent was distilled under reduced pressure and the crude residue redissolved in the minimum volume of a mixture of CH<sub>2</sub>Cl<sub>2</sub>/MeOH (1:1, v/v) before being applied on a column for chromatography (Al<sub>2</sub>O<sub>3</sub>, basic, grade I, 5 cm  $\times$  6 cm). Methanol is widely used for the column chromatography procedure because it has a dual effect on crude reaction mixtures: it solubilizes the succinimide and makes its elution faster and easier while the halogenated product, which is slightly soluble in that solvent, remains at the top of the column. *Note:* An alternative method for succinimide removal from the crude reaction mixture might be the treatment of the crude reaction residue in methanol with a subsequent filtration. However, the solution was found to contain minor amounts of the chlorinated products together with the vast majority of succinimide. The presence of the chlorinated porphyryns was manifested by the

characteristic Soret band. To minimize possible loss of the desired product(s), the following chromatographic procedure was applied. Elution of the excess of the chlorinated agent is achieved by pure MeOH. The first fraction, with dark brown color due to the large amount of decomposed succinimide, is eluted rapidly together with small amounts of partially halogenated porphyryns. The major part of porphyryns eluted only when the CH<sub>2</sub>Cl<sub>2</sub>/MeOH mixture is applied as eluant. Using a mixture of solvents, CH<sub>2</sub>Cl<sub>2</sub>/MeOH (0.01–0.2:1 v/v), several chlorinated side products, as dark green fractions, with Soret bands having  $\lambda_{\text{max}}$  values smaller than 425 nm, were removed. This is indicative for the lower degree of peripherally chlorinated porphyryns. No fraction with a  $\lambda_{\text{max}}$  bigger than 425 nm was obtained, or the concentration of such products is so small that they could not be detected by UV-vis spectroscopy. The gradual increase of CH<sub>2</sub>Cl<sub>2</sub> in solvent mixtures facilitates the elution of these partially chlorinated porphyryns as green fractions. The desired product, Ni(Cl<sub>4</sub>TPP), was eluted with CH<sub>2</sub>Cl<sub>2</sub>, CHCl<sub>3</sub>, or PhCH<sub>3</sub>. The solvents were evaporated under vacuum, the solid was redissolved in CH<sub>2</sub>Cl<sub>2</sub>/MeOH (1:1, v/v), and the chromatographic procedure was repeated using a column of 5 cm  $\times$  12 cm with the same solvents, except methanol, in the same order as described. The resulting product recrystallized from CH<sub>2</sub>Cl<sub>2</sub>/MeOH (1:5, v/v). Yield: 31%. <sup>1</sup>H NMR (CDCl<sub>3</sub>, 250 MHz):  $\delta$  = 8.65–8.85 (multiplet, 4H, pyr), 8.05–8.20 (multiplet, 8H, *o*-H<sub>phenyl</sub>), 7.75–8.00 (multiplet, 12H, *m*-H<sub>phenyl</sub> and *p*-H<sub>phenyl</sub>). MS (MALDI-TOF):  $m/z$  809 [M]<sup>+</sup>. Anal. Calcd for C<sub>44</sub>H<sub>24</sub>Cl<sub>4</sub>N<sub>4</sub>Ni: C, 65.31; H, 2.99; Cl, 17.52; N, 6.92. Found: C, 65.05; H, 3.21; Cl, 16.97; N, 6.45.

**$\beta$ -Octachloro-5,10,15,20-tetraphenylporphinato Nickel, 2.** To a solution of 1.0 g (1.50 mmol) of Ni(TPP) in 60 mL of 1,2-*o*-dichlorobenzene was added 2.4 g (18.0 mmol) *N*-chlorosuccinimide. The solution was brought to reflux for 2–3 h, and the reaction was monitored using UV-vis spectroscopy (the Soret band shifted from 411 to 439 nm). The purification/isolation procedure applied for the octachlorinated and octabrominated derivatives is similar to that described for the analogous tetrahalogenated porphyryns, but usually, one column chromatography procedure carried out on a 5 cm  $\times$  12 cm column is adequate for the isolation of analytically pure octachlorinated porphyryns. Column package has been performed with CH<sub>2</sub>Cl<sub>2</sub>/MeOH (1:1, v/v) mixtures as in the case of tetrahalogenated derivatives. The pure MeOH as eluant is followed by CH<sub>2</sub>Cl<sub>2</sub>/MeOH mixtures with initial volume in CH<sub>2</sub>Cl<sub>2</sub> higher than that used in the case of tetrahalogenated derivatives. That facilitates the elution of undesired partially halogenated porphyryns (the octachlorinated product is rather difficult to elute from the top of the column when the volume of CH<sub>2</sub>Cl<sub>2</sub> is less than in 50%, v/v, for the eluant). Thus, elution of porphyryns with less than eight chlorines could start with CH<sub>2</sub>Cl<sub>2</sub>/MeOH (0.3:1, v/v), yielding green fractions, and that holds even for solvent mixtures 50%–60% in CH<sub>2</sub>Cl<sub>2</sub>. Under these conditions, only fractions with  $\lambda_{\text{max}}$  smaller than 439 nm were collected. Using pure CH<sub>2</sub>Cl<sub>2</sub>, CHCl<sub>3</sub>, or PhCH<sub>3</sub> the desired octachlorinated compound is eluted. Purple crystals of the Ni(Cl<sub>8</sub>TPP) suitable for X-ray structure analysis were obtained. Yield: 70%. <sup>1</sup>H NMR (CDCl<sub>3</sub>, 250 MHz):  $\delta$  = 7.90–8.00 (multiplet, 8H, *o*-H<sub>phenyl</sub>), 7.65–7.80 (multiplet, 12H, *m*-H<sub>phenyl</sub> and *p*-H<sub>phenyl</sub>). MS (MALDI-TOF):  $m/z$  947 [M]<sup>+</sup>. Anal. Calcd for C<sub>44</sub>H<sub>20</sub>Cl<sub>8</sub>N<sub>4</sub>Ni: C, 55.81; H, 2.13; Cl, 29.95; N, 5.92. Found: C, 55.65; H, 2.21; Cl, 29.97; N, 5.80.

**$\beta$ -Tetrabromo-5,10,15,20-tetraphenylporphinato Nickel, 3.** To a solution of 1.0 g (1.50 mmol) of Ni(TPP) in 60 mL of 1,2-*o*-dichlorobenzene was added 1.067 g (6.0 mmol) of *N*-bromosuccinimide. The solution was brought to reflux for 2 h, and the reaction was followed by UV-vis spectroscopy. During the course

(69) Perrin, D. D.; Armarego, W. L. F. *Purification of Laboratory Chemicals*, 3rd ed.; Pergamon Press: New York, 1988; p 105.

(70) Fuhrhop, J. H.; Smith, K. M. *Porphyryns and Metalloporphyryns*; Elsevier Scientific Publishing Co.: Amsterdam, 1975; Section H, p 757.

of the reaction, the Soret band was shifted from 411 to 430 nm. The purification/isolation procedure followed was identical to that described previously for the tetrachlorinated derivative. Yield: 35%.  $^1\text{H NMR}$  ( $\text{CDCl}_3$ , 250 MHz):  $\delta = 8.75\text{--}9.0$  (multiplet, 4H, pyr), 8.15–8.3 (multiplet, 8H, *o*- $\text{H}_{\text{phenyl}}$ ), 7.80–8.00 (multiplet, 12H, *m*- $\text{H}_{\text{phenyl}}$  and *p*- $\text{H}_{\text{phenyl}}$ ). MS (MALDI-TOF):  $m/z$  987  $[\text{M}]^+$ . Anal. Calcd for  $\text{C}_{44}\text{H}_{24}\text{Br}_4\text{N}_4\text{Ni}$ : C, 53.54; H, 2.45; Br, 32.38; N, 5.68. Found: C, 53.05; H, 3.00; Br, 31.95; N, 6.05.

**$\beta$ -Octabromo-5,10,15,20-tetraphenylporphinato Nickel, 4.** To a solution of 1.0 g (1.50 mmol) of Ni(TPP) in 60 mL of 1,2-*o*-dichlorobenzene was added 3.204 g (18.0 mmol) of *N*-bromosuccinimide. The solution was brought to reflux for 2–3 h, and the reaction was monitored by UV–vis spectroscopy. During the course of the reaction, the Soret band was shifted from 411 to 449 nm and the Ni( $\text{Br}_8\text{TPP}$ ) purified as described previously. Yield: 85%.  $^1\text{H NMR}$  ( $\text{CDCl}_3$ , 250 MHz):  $\delta = 8.00\text{--}8.10$  (multiplet, 8H, *o*- $\text{H}_{\text{phenyl}}$ ), 7.75–7.90 (multiplet, 12H, *m*- $\text{H}_{\text{phenyl}}$  and *p*- $\text{H}_{\text{phenyl}}$ ). MS (MALDI-TOF):  $m/z$  1302.5  $[\text{M}]^+$ . Anal. Calcd for  $\text{C}_{44}\text{H}_{20}\text{Br}_8\text{N}_4\text{Ni}$ : C, 40.57; H, 1.55; Br, 49.07; N, 4.30. Found: C, 40.65; H, 1.70; Br, 49.00; N, 4.42.

**Demetalation of  $\beta$ -Octahalogeno-5,10,15,20-tetraphenylporphinato Nickel (X = Cl, Br and  $n = 4$  or 8).** A 400 mg portion of any Ni( $\text{X}_n\text{TPP}$ ) derivative was suspended in 100 mL of  $\text{CH}_2\text{Cl}_2$ , into a round-bottom flask, while 30 mL of  $\text{H}_2\text{SO}_4$  (98%) was added with great care. The mixture was rigorously stirred for 3–4 h at room temperature, and the progress of the demetalation was followed by UV–vis spectroscopy and by TLC plates. After the end of the reaction, the flask was transferred to an ice bath, and  $\text{NH}_3$  solution (25%) was added dropwise, under great precaution, to avoid overheating and violent boiling/evaporation of the organic solvent. The mixture was extracted several times with  $\text{H}_2\text{O}$  and washed with a saturated solution of  $\text{NaHCO}_3$  until pH 7.0. The organic phase dried for 45 min–1 h on  $\text{MgSO}_4$  and evaporated under vacuum. The crude product was redissolved in minimum volume of a mixture of  $\text{CH}_2\text{Cl}_2/\text{MeOH}$  (1:3, v/v) and applied on a column for chromatography ( $\text{Al}_2\text{O}_3$ , basic, grade I, 5 cm  $\times$  10 cm) using as eluant solvent mixtures such as  $\text{CH}_2\text{Cl}_2/\text{MeOH}$  (0.01–0.5:1, v/v). Analytically pure tetra- and octahalogenated free bases were obtained by using  $\text{CH}_2\text{Cl}_2$  as eluant. The solvents were evaporated and the products recrystallized from  $\text{CH}_2\text{Cl}_2/\text{MeOH}$  (1:5, v/v). Dark green crystals of  $\text{H}_2(\text{X}_8\text{TPP})\cdot 2\text{DMF}$  suitable for X-ray crystal structure analysis were obtained by slow diffusion of DMF into a saturated solution of the porphyrin in  $\text{PhCH}_3$  and simultaneous slow evaporation at room temperature.

**$\beta$ -Tetrachloro-5,10,15,20-tetraphenylporphyrin, 5.** Yield: 78%.  $^1\text{H NMR}$  ( $\text{CDCl}_3$ , 250 MHz):  $\delta = 8.65\text{--}8.75$  (multiplet, 4H, pyr), 8.00–8.10 (multiplet, 8H, *o*- $\text{H}_{\text{phenyl}}$ ), 7.60–7.80 (multiplet, 12H, *m*- $\text{H}_{\text{phenyl}}$  and *p*- $\text{H}_{\text{phenyl}}$ ), –2.80 (doublet, 2H, N–H). Anal. Calcd for  $\text{C}_{44}\text{H}_{26}\text{Cl}_4\text{N}_4$ : C, 70.23; H, 3.48; Cl, 18.84; N, 7.45. Found: C, 70.50; H, 3.71; Cl, 17.97; N, 7.85.

**$\beta$ -Octachloro-5,10,15,20-tetraphenylporphyrin, 6.** Yield: 88%.  $^1\text{H NMR}$  ( $\text{CDCl}_3$ , 250 MHz):  $\delta = 8.10\text{--}8.15$  (multiplet, 8H, *o*- $\text{H}_{\text{phenyl}}$ ), 7.70–7.80 (multiplet, 12H, *m*- $\text{H}_{\text{phenyl}}$  and *p*- $\text{H}_{\text{phenyl}}$ ), 1.55 (broad, 2H, N–H). Anal. Calcd for  $\text{C}_{44}\text{H}_{22}\text{Cl}_8\text{N}_4$ : C, 59.36; H, 2.49; Cl, 31.86; N, 6.29. Found: C, 59.50; H, 2.70; Cl, 31.97; N, 6.50.

**$\beta$ -Tetrabromo-5,10,15,20-tetraphenylporphyrin, 7.** Yield: 71%.  $^1\text{H NMR}$  ( $\text{CDCl}_3$ , 250 MHz):  $\delta = 8.70\text{--}8.85$  (multiplet, 4H, pyr), 8.05–8.15 (multiplet, 8H, *o*- $\text{H}_{\text{phenyl}}$ ), 7.60–7.80 (multiplet, 12H, *m*- $\text{H}_{\text{phenyl}}$  and *p*- $\text{H}_{\text{phenyl}}$ ), –2.85 (doublet, 2H, N–H). Anal. Calcd for  $\text{C}_{44}\text{H}_{26}\text{Br}_4\text{N}_4$ : C, 56.81; H, 2.82; Br, 34.36; N, 6.02. Found: C, 56.50; H, 2.51; Br, 34.52; N, 6.00.

**$\beta$ -Octabromo-5,10,15,20-tetraphenylporphyrin, 8.** Yield: 82%.  $^1\text{H NMR}$  ( $\text{CDCl}_3$ , 250 MHz):  $\delta = 8.40\text{--}8.50$  (multiplet, *o*- $\text{H}_{\text{phenyl}}$ ),

7.90–8.00 (multiplet, 12H, *m*- $\text{H}_{\text{phenyl}}$  and *p*- $\text{H}_{\text{phenyl}}$ ), 1.25 (doublet, 2H, N–H). Anal. Calcd for  $\text{C}_{44}\text{H}_{22}\text{Br}_8\text{N}_4$ : C, 42.42; H, 1.78; Br, 51.31; N, 4.50. Found: C, 42.60; H, 1.70; Br, 51.37; N, 4.70. *Note:* Addition of small amounts of  $\text{D}_2\text{O}$  in the NMR tube of all the porphyrin samples results in the disappearance of the exchangeable N–H protons, thus verifying in the case of derivatives **6** and **8** the significant downfield shift of those protons with respect to the tetrahalogenated porphyrins.

**$\beta$ -Tetrahalogeno-5,10,15,20-tetraphenylporphinato Terbium (Acetato) 9 and 11 (X = Cl, Br).** To a solution of 150 mg of  $\text{H}_2(\text{X}_4\text{TPP})$  (0.20 mmol for X = Cl and 0.16 mmol for X = Br) was added 300 mg (0.6 mmol) of  $\text{Tb}(\text{acac})_3\cdot\text{H}_2\text{O}$  in a round-bottom flask containing 20 mL of 1,2,4-trichlorobenzene. The solution was brought to reflux for 3–4 h. The reaction was monitored by UV–vis spectroscopy, and the Soret band was red-shifted from 426–430 to 431–432 nm. After the end of the reaction, the solvent was distilled under reduced pressure and the crude residue redissolved in the minimum volume of  $\text{PhCH}_3$  before the mixture was applied on a column for chromatography ( $\text{Al}_2\text{O}_3$ , basic, grade I, 3 cm  $\times$  5 cm). The unreacted free base is eluted easily from the top of the column while  $\text{CH}_2\text{Cl}_2$  and  $\text{CH}_2\text{Cl}_2/\text{MeOH}$  (1:0.1–1, v/v) were used as solvent mixtures. Thus, the complete elution of the free porphyrin is achieved, and the elution of the terbium complexes started. Using as eluant pure MeOH and MeOH/DMSO (2:1, v/v) mixtures, the elution procedure is accelerated, and the complexes were recovered. The solvents were removed under reduced pressure, and the solid residue is recrystallized from  $\text{PhCH}_3$  or mixtures of  $\text{PhCH}_3/\text{petroleum ether}$  (1:5, v/v) yielding amorphous purple solid. After filtration, the solid is washed with cold petroleum and diethyl ether and dried for 2–3 days under vacuum at 40 °C. Total yields: **9**, 48%; **11**, 55%. Anal. Calcd for **9** ( $\text{Me}_2\text{SO}$ ) $_2$   $\text{C}_{50}\text{H}_{39}\text{Cl}_4\text{N}_4\text{O}_4\text{S}_2\text{Tb}$ : C, 53.39; H, 3.50; Cl, 12.61; N, 4.98. Found: C, 52.90; H, 3.44; Cl, 13.02; N, 5.10. Calcd for **11** ( $\text{Me}_2\text{SO}$ ) $_2$   $\text{C}_{50}\text{H}_{39}\text{Br}_4\text{N}_4\text{O}_4\text{S}_2\text{Tb}$ : C, 46.11; H, 3.02; Br, 24.54; N, 4.30. Found: C, 46.03; H, 3.04; Cl, 24.64; N, 4.34.

**$\beta$ -Octahalogeno-5,10,15,20-tetraphenylporphinato Terbium (Acetato) 10 and 12 (X = Cl, Br).** To a solution of 300 mg of  $\text{H}_2(\text{X}_8\text{TPP})$  (0.33 mmol for X = Cl and 0.24 mmol for X = Br) was added 300 mg (0.6 mmol) of  $\text{Tb}(\text{acac})_3\cdot\text{H}_2\text{O}$  in a round-bottom flask containing 20 mL of 1,2,4-trichlorobenzene. The solution was brought to reflux for 3–4 h. The reaction was monitored by UV–vis spectroscopy, and the Soret band was red-shifted from 453 or 469 nm (for X = Cl and X = Br, respectively) to 458–460 nm (X = Cl) and 473–474 nm (X = Br). After the end of the reaction, the solvent was distilled under reduced pressure. The purification and isolation of the complexes was carried out in an identical way to that described for the  $\beta$ -tetrahalogenated derivatives. The complexes are recrystallized either from saturated  $\text{PhCH}_3$  solutions or from mixtures of  $\text{PhCH}_3/\text{petroleum ether}$  (1:5, v/v) and dried for 2–3 days under vacuum at 40 °C. Total yields: **10**, 70%; **12**, 66%. Green crystals suitable for X-ray crystal analysis,  $\text{Tb}(\text{Cl}_8\text{TPP})(\text{OAc})(\text{DMSO})_2$ , were recovered after slow evaporation of  $\text{PhCH}_3$  solution. Anal. Calcd for **10** ( $\text{Me}_2\text{SO}$ ) $_2$   $\text{C}_{50}\text{H}_{35}\text{Cl}_8\text{N}_4\text{O}_4\text{S}_2\text{Tb}$ : C, 47.57; H, 2.79; Cl, 22.46; N, 4.44. Found: C, 47.91; H, 2.90; Cl, 22.28; N, 4.45. Calcd for **12** ( $\text{Me}_2\text{SO}$ ) $_2$   $\text{C}_{50}\text{H}_{35}\text{Br}_8\text{N}_4\text{O}_4\text{S}_2\text{Tb}$ : C, 37.11; H, 2.18; Br, 39.50; N, 3.46. Found: C, 36.91; H, 2.22; Br, 39.40; N, 3.42.

**X-ray Structure Determination.** A green crystal of Ni( $\text{Cl}_8\text{TPP}$ ) (0.10  $\times$  0.20  $\times$  0.50 mm $^3$ ) was mounted on a  $P2_1$  Nicolet diffractometer upgraded by Crystal Logic and measured using Zr-filtered Mo radiation. A flat octahedral dark green crystal of  $\text{H}_2(\text{Br}_8\text{TPP})\cdot 2\text{DMF}$  (0.20  $\times$  0.40  $\times$  0.40 mm $^3$ ) and a deep purple crystal of  $\text{Tb}(\text{Cl}_8\text{TPP})(\text{OAc})(\text{DMSO})_2\cdot 3\text{PhCH}_3\cdot\text{MeOH}$  (0.08  $\times$  0.12  $\times$  0.50

**Table 1.** Crystal Data for Ni(Cl<sub>8</sub>TPP), H<sub>2</sub>(Br<sub>8</sub>TPP)·2DMF, and Tb(Cl<sub>8</sub>TPP)(OAc)(DMSO)<sub>2</sub>·3PhCH<sub>3</sub>·MeOH

	Ni(Cl <sub>8</sub> TPP)	H <sub>2</sub> (Br <sub>8</sub> TPP)·DMF	Tb complex
formula	C <sub>44</sub> H <sub>20</sub> Cl <sub>8</sub> N <sub>4</sub> Ni	C <sub>50</sub> H <sub>36</sub> Br <sub>8</sub> N <sub>6</sub> O <sub>2</sub>	C <sub>72</sub> H <sub>63</sub> Cl <sub>8</sub> N <sub>4</sub> O <sub>5</sub> S <sub>2</sub> Tb
fw	946.95	1392.16	1570.91
temp, K	298	298	298
λ, Å	Mo Kα, 0.71073	Mo Kα, 0.71073	Mo Kα, 0.71073
a, Å	10.727(1)	20.59(1)	19.776(5)
b, Å	27.014(4)		13.516(3)
c, Å	14.423(2)	10.935(6)	30.015(6)
β	111.168(3)		108.409(7)
V, Å <sup>3</sup>	3897.6(9)	4637(4)	7612(3)
Z	4	4	4
space group	P2 <sub>1</sub> /a	I4 <sub>1</sub> /a	P2 <sub>1</sub> /c
D <sub>calcd</sub> , Mg m <sup>-3</sup>	1.614	1.994	1.371
μ, mm <sup>-1</sup>	1.074	6.965	1.271
GOF	1.110	1.049	1.126
R1	0.0569 <sup>a</sup>	0.0471 <sup>b</sup>	0.0754 <sup>c</sup>
wR2	0.0875 <sup>a</sup>	0.1164 <sup>b</sup>	0.2080 <sup>c</sup>

<sup>a</sup> For 2493 reflections with  $I > 2\sigma(I)$ . <sup>b</sup> For 1996 reflections with  $I > 2\sigma(I)$ . <sup>c</sup> For 6363 reflections with  $I > 2\sigma(I)$ .

mm<sup>3</sup>) were mounted in air and covered with epoxy glue. Diffraction measurements were made on a Crystal Logic Dual Goniometer diffractometer using graphite monochromated Mo radiation. Unit cell dimensions for the three structures were determined and refined by using the angular settings of 25 automatically centered reflections in the range  $11^\circ < 2\theta < 23^\circ$ , and they appear in Table 1. Intensity data were recorded using a  $\theta$ - $2\theta$  scan. Three standard reflections monitored every 97 reflections showed less than 3% variation and no decay. Lorentz, polarization, and  $\psi$ -scan absorption corrections were applied using Crystal Logic software. The structures were solved by direct methods using SHELXS-86<sup>71</sup> and refined by full-matrix least-squares techniques on  $F^2$  with SHELXL-93.<sup>72</sup> Supplementary crystal data for Ni(Cl<sub>8</sub>TPP) are the following:  $2\theta_{\max} = 47^\circ$ , scan speed 1.5°/min, scan range  $2.4 + \alpha_1\alpha_2$  separation, reflections collected/unique/used = 5733/5379 ( $R_{\text{int}} = 0.0649$ )/5368, 594 parameters refined, R1/wR2 (for all data) = 0.0786/0.1375,  $[\Delta/\sigma]_{\max} = 0.007$ ,  $[\Delta\rho]_{\max}/[\Delta\rho]_{\min} = 0.406/-0.371 \text{ e}/\text{\AA}^3$ . All hydrogen atoms were located by difference maps and their positions refined isotropically. All nonhydrogen atoms were refined anisotropically. For H<sub>2</sub>(Br<sub>8</sub>TPP)·2DMF, the data are the following:  $2\theta_{\max} = 50^\circ$ , scan speed 1.0°/min, scan range  $2.5 + \alpha_1\alpha_2$  separation, reflections collected/unique/used = 2114/1996 ( $R_{\text{int}} = 0.0495$ )/1991, 157 parameters refined, R1/wR2/GOF (for all data) = 0.0864/0.1392,  $[\Delta/\sigma]_{\max} = 0.194$ ,  $[\Delta\rho]_{\max}/[\Delta\rho]_{\min} = 0.677/-0.476 \text{ e}/\text{\AA}^3$ . All hydrogen atoms (except those of N<sub>1</sub> and C<sub>10</sub> which were introduced at calculated positions as riding on bonded atoms) were located by difference maps and refined isotropically. All non-hydrogen atoms refined anisotropically, but the atoms of the solvents refined isotropically. For Tb(Cl<sub>8</sub>TPP)(OAc)(DMSO)<sub>2</sub>·3PhCH<sub>3</sub>·MeOH, the data are the following:  $2\theta_{\max} = 44.3^\circ$ , scan speed 1.0°/min, scan range  $2.3 + \alpha_1\alpha_2$  separation, reflections collected/unique/used = 8864/8658 ( $R_{\text{int}} = 0.0192$ )/8641, 696 parameters refined, R1/wR2/GOF (for all data) = 0.1106/0.2630,  $[\Delta/\sigma]_{\max} = 0.882$ ,  $[\Delta\rho]_{\max}/[\Delta\rho]_{\min} = 2.498/-1.729 \text{ e}/\text{\AA}^3$  in the vicinity of the heavy metal. All hydrogen atoms were introduced at calculated positions as riding on bonded atoms. All non-hydrogen atoms were refined anisotropically, except those of the solvent molecules which were refined isotropically. The phenyl ring of one toluene solvent molecule was fixed to a regular hexagon and its occupation factor

fixed to 0.50; the solvent methanol was refined with occupation factor fixed to 0.25.

## Results

Modifying known protocols, we achieved the high-yield synthesis of brominated and chlorinated Ni derivatives of 5,10,15,20-tetraphenylporphyrin, bearing four or eight halogens at  $\beta$ -pyrrole positions. The demetalation of the Ni compounds yielded the free porphyrins which are then reacted with the acetylacetonato salt of Tb leading to the first lanthanide complexes with polyhalogenated and distorted porphyrins. The physicochemical properties of the halogenated compounds are studied by UV-vis and <sup>1</sup>H NMR spectroscopy and electrochemical methods. An attempt to understand the consequences of the number and nature of the halogen atoms, as well as to clarify the impact of presence and the nature of the metal ion on the physicochemical properties of the compounds, is presented in the following section. The afforded X-ray structure of Ni(Cl<sub>8</sub>TPP) is described, and the structural features are discussed and compared with Ni complexes of other polyhalogenated porphyrin macrocycles as well as with the Tb octachloro complex. The structural characteristics of the previously communicated X-ray structure of the octabrominated free base<sup>29</sup> are also presented and compared with the structures of the other halogenated compounds described in this work.

## Discussion

**Synthesis.** Traylor and Tsuchiya<sup>8</sup> reported for the first time the bromination of Zn tetrakis(2,6-dichlorophenyl) porphyrin by action with *N*-bromosuccinimide (NBS). All the halogenated porphyrins reported herein were prepared according to the experimental procedure reported by Dolphin and co-workers<sup>17,37</sup> for the synthesis of  $\beta$ -octachloro tetrakis(2,6-dichlorophenyl) porphyrin. However, no attempts have been reported, as far as we know, for the synthesis of  $\beta$ -tetrabromo-,  $\beta$ -tetrachloro-, or  $\beta$ -octabromo-tetraphenylporphyrins via an NBS/NCS protocol. The only protocol still used for the bromination of tetraphenylporphyrin is that reported by Bhyrappa and Krishnan.<sup>33</sup> Our attempts to achieve the synthesis of hyperbrominated porphyrin rings led to a synthetic protocol which is remarkably fast and simple compared to that for the Cu derivative<sup>33,73</sup> and exhibits the advantage that gives the desired products in higher yields (up to 85%). However, the reaction time required for the demetalation of the nickel derivative is slightly longer.

For the synthesis of the nickel  $\beta$ -tetrahalogenated derivatives (**1** and **3**, Chart 1), the same experimental conditions were used (see also Experimental Section) and should yield products with one halogen in each pyrrole ring,<sup>29</sup> according to extensive studies reported by Crossley et al.<sup>74</sup> This lack of stereospecificity is rationalized by the predominant absence of localized double-bond character in the metal derivatives, instead of the free base. This suggests the introduction of one halogen atom in each pyrrolic/pyrrolic

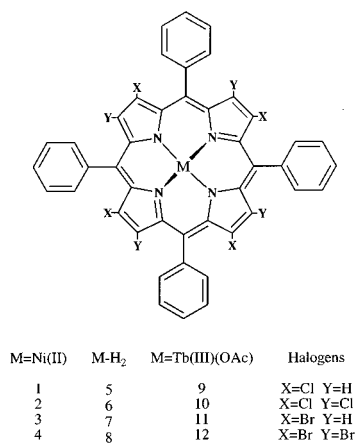
(71) Sheldrick, G. M. *SHELXS-86: Structure Solving Program*; University of Göttingen: Germany, 1986.

(72) Sheldrick, G. M. *SHELXL-93: Crystal Structure Refinement*; University of Göttingen: Germany, 1993.

(73) Spyroulias, G. A.; Coutsolelos, A. G. *Polyhedron* **1995**, *14*, 2483.

(74) Crossley, M. J.; Burn, P. L.; Chew, S. S.; Cuttance, F. B.; Newson, I. A. *J. Chem. Soc., Chem. Commun.* **1991**, 1564.

Chart 1



ring instead of two halogens in the antipode pyrroles as has been reported for the  $\beta$ -tetrahalogenated tetramesitylporphyrin.<sup>75</sup>

However, the fact that multiple ill-resolved peaks corresponding to pyrrole proton resonances are observed by <sup>1</sup>H NMR spectroscopy data makes it unfeasible to determine whether any of the pyrrole proton signals split because of vicinal coupling, if there are any vicinal protons. This indicates that the four remaining pyrrole protons are unequivalent, suggesting that the halogenation procedure yields a mixture of isomers. Similar kinds of regioisomers are also observed in the case of thallium complexes of tetrachlorinated TPP and detected only through <sup>205</sup>Tl NMR spectroscopy.<sup>76</sup> Attempts to separate the mixture of compounds did not succeed because of their identical behavior on different chromatography material even when a variety of solvent mixtures was used as eluant. Thus, the exact composition of the mixture is rather difficult to detect. Nevertheless, no noticeable difference in physical properties associated with the magnitude of ring distortion should be anticipated because  $\beta$ -tetrasubstituted porphyrin cores are nearly planar.<sup>75</sup> This aspect is also supported by the electrooxidation potentials for  $\beta$ -tetrabromo- and chloro-TTP reported in this study (see also the Electrochemistry section). Oxidation potentials, which are rather sensitive to ring distortion,<sup>26</sup> exhibit  $E_{1/2}$  values almost identical to those of antipodal tetrahalogenated TMP,<sup>75</sup> indicating that various distribution/substitution patterns of four halogens on the pyrroles do not induce a different degree of ring distortion and consequently do not significantly influence the HOMO energy. Finally, it should be noted that the possibility of an isomeric substitution pattern was taken under consideration in the following discussion and evaluation of the experimental results.

Insertion of the Tb ion from Tb(acac)<sub>3</sub>·H<sub>2</sub>O into H<sub>2</sub>(X<sub>n</sub>TPP) in 1,2,4-tcb yields purple Tb(X<sub>4</sub>TPP)(OAc), **9** and **11**, (X = Cl, Br and n = 4) and deep purple Tb(X<sub>8</sub>TPP)(OAc), **10** and **12**, (X = Cl, Br and n = 8) compounds after 2–4 h. Purification and isolation of the lanthanide porphyrins have

been performed as described elsewhere (see also Experimental Section). All the compounds gave satisfactory elemental analysis, and the nature of the axial ligand has been identified by IR<sup>77</sup> spectroscopy and X-ray crystallographic studies. The pyrolysis of Tb(acac)<sub>3</sub>·H<sub>2</sub>O during the course of the high-temperature metalation reaction provides a reasonable explanation for the presence of the acetato ligand as axial ligand on the terbium ion.<sup>78–80</sup>

**UV–Vis Spectroscopy.** The number and the nature of the  $\beta$ -pyrrole substituents on the porphyrin core affect the structure and the spectroelectrochemical properties of the macrocycle. Semiempirical AM1 electronic structure calculations indicate that HOMO and LUMO orbitals are destabilized by the distortion of the ring when  $\beta$ -pyrrole hydrogens are replaced by other bulky substituents.<sup>21,26,81–83</sup> The electronic properties of the substituent groups, electron acceptors or electron donors, influence the properties of the porphyrin to a different extent. The halogenation of the porphyrin ring causes severe distortion to the ring, and as a consequence, the Soret absorption band is considerably shifted to lower energy while the Q bands are also shifted to lower energy but to a smaller extent (Table 2). According to the number of halogens inserted on the macrocyclic ring, the Soret band is bathochromically shifted from 20 nm when four halogens are inserted, **1** and **3**, to up to 40 nm (for eight halogens), **2** and **4**, in the Ni porphyrin complexes (Soret  $\lambda_{\text{max}}$  = 411 nm for Ni(TPP), CH<sub>2</sub>Cl<sub>2</sub>, 20 °C). The same bathochromic shift, though of a higher magnitude, is observed in the case of the free base porphyrins (Table 2). While the TPP free base presents a Soret  $\lambda_{\text{max}}$  at 417 nm (CH<sub>2</sub>Cl<sub>2</sub>, 20 °C), the Soret absorption in  $\beta$ -tetrahalogenated free porphyrins is bathochromically shifted to 426–430 nm (**5**, **7**) and to 453 and 469 nm for the  $\beta$ -octachloro- and bromosubstituted porphyrins (**6**, **8**), respectively. Finally, comparable shifts experience the Soret absorption in the case of Tb porphyrin complexes (Soret  $\lambda_{\text{max}}$  = 420 nm for Tb(TPP)(acac), CH<sub>2</sub>Cl<sub>2</sub>, 20 °C) (Table 2). The number of halogens in  $\beta$  pyrrole positions, in addition to the dramatic effect on the transition energy of the Soret band, influences the number and the nature of Q bands as well. In the case of the Ni complexes, the spectra present the typical absorption for the Ni complex in the region of Q bands (540 and 543 nm for the  $\beta$ -tetra and 553 and 561 nm for the  $\beta$ -octachloro and -bromo derivatives, respectively (Table 2)). A weak absorption band, rather a shoulder, is also observed at a lower transition energy than the main Q band, around 580–600 nm. However, the spectral features observed for the free

(75) Ochsenbein, P.; Ayougou, K.; Mandon, D.; Fischer, J.; Weiss, R.; Austin, R. N.; Jayaraj, K.; Gold, A.; Terner, J.; Fajer, J. *Angew. Chem., Int. Ed. Engl.* **1994**, *33*, 348.

(76) Coutsolelos, A. G.; Daphnomili, D. *Inorg. Chem.* **1997**, *36*, 4614.

(77) For all the Tb halogenated porphyrins characteristic bands observed in the area of 1440–1446 and 1490–1496 cm<sup>-1</sup> attributable to O<sub>2</sub>-CMe, bidentate coordination of the acetato ligand is indicated.<sup>29</sup>

(78) Wong, C.-P.; Veintecher, R. F.; Horrocks, D. W., Jr. *J. Am. Chem. Soc.* **1974**, *96*, 7149.

(79) Wong, C.-P.; Horrocks, D. W., Jr. *Tetrahedron Lett.* **1975**, 2637.

(80) Buchler, J. W.; Eickelmann, G.; Puppe, L.; Rohbock, K.; Schneehage, H. H.; Weck, D. *Liebigs Ann. Chem.* **1971**, *745*, 135.

(81) Barkigia, K. M.; Chantranupong, L.; Smith, K. M.; Fajer, J. *J. Am. Chem. Soc.* **1988**, *110*, 7566.

(82) Gassman, P. G.; Ghosh, A.; Almlof, J. *J. Am. Chem. Soc.* **1992**, *114*, 9990.

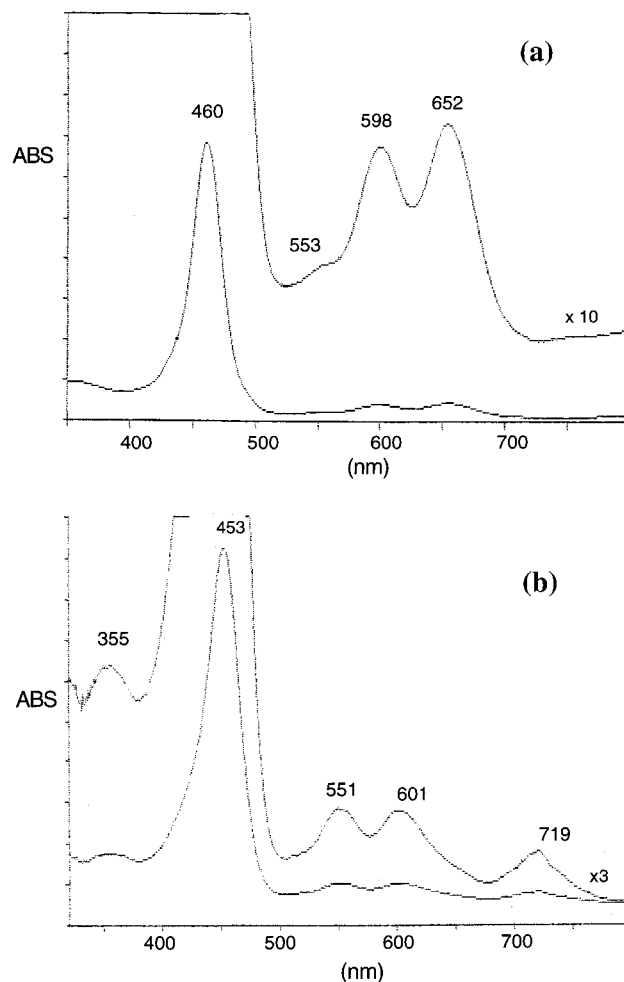
(83) Parusel, A. B. J.; Wondimagegn, T.; Ghosh, A. *J. Am. Chem. Soc.* **2000**, *122*, 6371–6374.

**Table 2.** UV–Vis Data for  $\beta$ -Tetra- and Octahalogenated Porphyrins  $M(X_n\text{TPP})$  in  $\text{CH}_2\text{Cl}_2$  Where  $M = \text{H}_2, \text{Ni},$  or  $\text{Tb}(\text{OAc})$ ,  $X = \text{Cl}$  or  $\text{Br}$ , and  $n = 4$  or  $8$  [ $\lambda_{\text{max}}/\text{nm}$ , ( $\log \epsilon \text{ dm}^{-3} \text{ mol}^{-1} \text{ cm}^{-1}$ )]

		B bands		Q bands	
Ni( $X_n\text{TPP}$ )					
Ni( $\text{Cl}_4\text{TPP}$ )	1	425		540	580(sh)
		5.68		3.00	
Ni( $\text{Cl}_8\text{TPP}$ )	2	439		553	587(sh)
		5.67		3.04	
Ni( $\text{Br}_4\text{TPP}$ )	3	430		543	581(sh)
		5.67		3.08	
Ni( $\text{Br}_8\text{TPP}$ )	4	449		561	599(sh)
		5.66		3.08	
$\text{H}_2(X_n\text{TPP})$					
$\text{H}_2(\text{Cl}_4\text{TPP})$	5	426	523	599	667
		5.44	4.54	3.56	3.54
$\text{H}_2(\text{Cl}_8\text{TPP})$	6	355	453	551	601
		4.30	5.38	4.04	4.03
$\text{H}_2(\text{Br}_4\text{TPP})$	7	430	527	598	673
		5.40	4.29	3.51	3.49
$\text{H}_2(\text{Br}_8\text{TPP})$	8	368	469	569	625
		4.48	5.31	4.02	4.14
$\text{Tb}(X_n\text{TPP})(\text{OAc})$					
$\text{Tb}(\text{Cl}_4\text{TPP})(\text{OAc})$	9	432	563	596	
		5.25	4.20	3.76	
$\text{Tb}(\text{Cl}_8\text{TPP})(\text{OAc})$	10	358	460	553	598
		4.33	4.77	3.69	3.85
$\text{Tb}(\text{Br}_4\text{TPP})(\text{OAc})$	11	432	569	596	
		5.20	4.15	3.64	
$\text{Tb}(\text{Br}_8\text{TPP})(\text{OAc})$	12	366	474	552	612
		4.40	4.65	3.48	3.42

bases exhibit striking differences with the halogen-free  $\text{H}_2$ -(TPP) precursor, manifested in the area of the Q bands. Specifically, both the tetrahalogenated derivatives present three Q bands instead of the four in the case of  $\text{H}_2(\text{TPP})$  (Figure 1). The two higher energy Q bands, slightly shifted compared to the analogous band in  $\text{H}_2(\text{TPP})$ ,<sup>84</sup> observed at 523, 599 nm (for  $\text{Cl}_4\text{TPP}$ ) and at 527, 598 nm (for  $\text{Br}_4\text{TPP}$ ), could be compared with the  $Q_y(1,0)$  and  $Q_x(1,0)$ , while the higher energy  $Q_y(1,0)$  seems to gain in intensity and the  $Q_y(0,0)$  band (which is observed in  $\text{H}_2(\text{TPP})$ ) is probably shifted to higher energy and could be observed as a shoulder to the  $Q_x(1,0)$  band (Figure 1). The lower energy Q band observed for the  $X_4\text{TPP}$  derivatives (where  $X = \text{Cl}$  or  $\text{Br}$ ) presents an unusual large value at 667 nm (for  $\text{Cl}_4\text{TPP}$ ) and 673 nm (for  $\text{Br}_4\text{TPP}$ ) compared with similar data reported in the case of the  $\beta$ -tetrahalogenated tetrakis(mesityl)porphyrin with two halogens on antipodal pyrroles.<sup>75</sup> The two octahalogenated porphyrins present rather similar optical features (Figure 1) that are (i) the high energy band at 355 and 368 nm (for  $\text{Cl}_8\text{TPP}$  and  $\text{Br}_8\text{TPP}$  respectively), (ii) the bathochromically shifted Soret absorption at 453 nm ( $\text{Cl}_8\text{TPP}$ ) and 469 nm ( $\text{Br}_8\text{TPP}$ ), and (iii) three Q bands, two at the area of 560–625 nm and the third at the area of 719–745 nm. The only observed difference between them lies in the intensity of the higher energy Q band, for which, in the case of the  $\beta$ -octachloroporphyrin (at 561 nm), the intensity is almost equal with the intensity of the Q band at 601 nm. In contrast,

(84)  $\text{H}_2(\text{TPP})$  exhibits four Q bands where its origin lies in the vibronic mixing resulting in the appearance of  $Q_y(1,0)$ ,  $Q_y(0,0)$ ,  $Q_x(1,0)$ , and  $Q_x(0,0)$  transitions in the order of decreasing energy and intensity. Gouterman, M. *The Porphyrins*; Dolphin, D., Ed.; Academic Press: New York, 1978; Vol. III, p 1. Those bands in  $\text{CH}_2\text{Cl}_2$ , 20 °C, appeared at 517, 550, 592, and 650 nm, respectively.

**Figure 1.** UV–vis spectra of (a)  $\text{H}_2(\text{Cl}_8\text{TPP})$  and (b)  $\text{Tb}(\text{Cl}_8\text{TPP})(\text{OAc})$  in  $\text{CH}_2\text{Cl}_2$ .

the intensity of the higher energy Q band of the  $\beta$ -octabromo compound (at 569 nm) is of significantly lower intensity compared with the Q band at 625 nm. The two tetrahalogenated Tb complexes exhibit rather similar spectral features with the TPP complexes (Table 2). The Soret absorption is red-shifted (432 nm), while three bands appeared at the area 550–600 nm with that at 569 nm exhibiting the higher intensity. However, this is not the case in the spectra of  $\text{Tb}(X_8\text{TPP})$  complexes. Three rather broad absorption bands were observed between 550 and 670 nm. In both octahalogenated porphyrins, the higher energy Q band (at 553 nm in both complexes) is of lower intensity while that of lower energy at 652 nm (for  $\text{Cl}_8\text{TPP}$  complex) and 669 nm (for  $\text{Br}_8\text{TPP}$  complex) exhibits the higher intensity among the three (Figure 1).

**Electrochemistry.** Cyclic voltammetry experiments for all the complexes were carried out in  $\text{CH}_2\text{Cl}_2$ , containing 0.1 M  $\text{NBu}_4\text{PF}_6$ . One reduction and one oxidation process was observed for each  $\text{H}_2(X_4\text{TPP})$  derivative, and two reduction and two oxidation waves were observed for the  $\text{H}_2(X_8\text{TPP})$  analogues. Under the same conditions, all the  $\text{Tb}(X_n\text{TPP})(\text{OAc})$  complexes manifest two reduction and three oxidation processes. All of the described electrochemical reactions are reversible and, in each case, correspond to one-electron

**Table 3.** Half-Wave Potentials (V vs SCE) for Oxidation and Reduction of  $\beta$ -Tetra- and Octahalogenated Porphyrins  $M(X_n\text{TPP})X$  (where  $M = \text{H}_2$  or  $\text{Tb}(\text{OAc})$ ,  $X = \text{Cl}$  or  $\text{Br}$  and  $n = 4$  or  $8$ ) in  $\text{THF}/\text{NBu}_4\text{ClO}_4$  0.1 M (V vs SCE)

porphyrin		$E_{1/2}$ 2nd red	$E_{1/2}$ 1st red	$E_{1/2}$ 1st ox	$E_{1/2}$ 2nd ox	$E_{1/2}$ 3rd ox	HOMO–LUMO	Soret $\lambda_{\text{max}}$ (nm)
$\text{H}_2(\text{Cl}_4\text{TPP})$	<b>1</b>	<i>a</i>	–1.10	1.12	<i>a</i>	<i>a</i>	2.22	426
$\text{H}_2(\text{Cl}_8\text{TPP})$	<b>2</b>	–1.11	–0.83	1.04	1.26	<i>a</i>	1.87	456
$\text{H}_2(\text{Br}_4\text{TPP})$	<b>3</b>	<i>a</i>	–1.02	1.05	<i>a</i>	<i>a</i>	2.07	430
$\text{H}_2(\text{Br}_8\text{TPP})$	<b>4</b>	–1.18	–0.77	0.93	1.17	<i>a</i>	1.70	462
$\text{Tb}(\text{Cl}_4\text{TPP})(\text{OAc})$	<b>9</b>	–1.22	–1.00	0.98	1.19	1.57	1.98	430
$\text{Tb}(\text{Cl}_8\text{TPP})(\text{OAc})$	<b>10</b>	–1.17	–0.87	1.03	1.26	1.63	1.90	460
$\text{Tb}(\text{Br}_4\text{TPP})(\text{OAc})$	<b>11</b>	–1.03	–0.93	0.81	1.10	1.49	1.74	432
$\text{Tb}(\text{Br}_8\text{TPP})(\text{OAc})$	<b>12</b>	–1.04	–0.86	0.86	<i>b</i>	<i>b</i>	1.72	474

<sup>a</sup> Not observed. <sup>b</sup> Not measured/ill-defined redox couple.

transfer. The electron withdrawing character of the bromine and chlorine substituents is expected to influence significantly the electrochemical properties of the porphyrinic derivatives. Consequently, the presence of these groups at  $\beta$ -pyrrole positions stabilizes both the HOMOs and the LUMOs with respect to those of the unsubstituted derivatives. Thus, the chloro- or bromosubstituted porphyrins would be easier to reduce and harder to oxidize, and the ring-centered electro-reductions should shift anodically with respect to their precursors. So, the more substituted the pyrrole ring is with halogen, the harder it would be to oxidize because of the more electron deficient character of the halogenated porphyrin ring. Nevertheless, this is not the case (Table 3). As has been theoretically<sup>83,85</sup> and experimentally<sup>82</sup> demonstrated, one must also consider the steric constraints caused by addition of up to eight bulky groups on  $\beta$ -pyrrolic positions, like Cl and Br, which strongly modify the redox properties due to the ring deformation.<sup>83</sup> The observation is in agreement with the reported systematic electrochemical study of iron porphyrins  $\text{Fe}(\text{Br}_n\text{TPP})\text{Cl}$  (where  $n = 0, 1, 2, \dots, 8$ ) by Kadish and co-workers,<sup>26,86</sup> where it has been proven that for 1–3 bromine substituents the redox potentials are governed by the induction effect. In contrast, for 4 up to 8 bromines, the reduction potential is still governed by the inductive effects, while in the case of the oxidation potentials the distortion dominates the inductive effect. Because macrocycle distortion destabilizes the HOMOs, leaving the LUMOs relatively unchanged (slight stabilization), and the destabilizing effect on the HOMOs predominates in the severely distorted octahalogenosubstituted porphyrins, they are not only easier to oxidize than the tetrahalogeno compounds, but they are also easier to reduce. However, at this point, it should be noted that because the molecular structures of tetrahalogenated tetraphenylporphyrins have not been determined, and isomers with unknown distribution of the four halogens should be considered, a quantitative evaluation of the distortion effect in the redox properties of the compounds is rather difficult. Insights for the molecular structures of tetrahalogenated compounds are provided and taken into account in the discussion that follows, by the crystal structures of almost planar tetrabromo- and tetrachlorotetramesitylporphyrins with the two halogens sited in antipodal pyrroles. Regarding the redox potentials, listed in Table 3, it is evident

that the  $\text{H}_2(\text{X}_4\text{TPP})$  derivatives are more difficult to reduce and oxidize, relative to the  $\text{H}_2(\text{X}_8\text{TPP})$  analogues. This is in good agreement with the reported data of Kadish mentioned previously.<sup>26,86</sup> Furthermore, in agreement with recently published data, the  $E_{1/2}(\text{1st-ox}) - E_{1/2}(\text{1st-red})$  or HOMO–LUMO gaps of the  $\text{H}_2(\text{Br}_n\text{TPP})$  derivatives are smaller than those of the corresponding chlorinated compounds.<sup>75</sup> The  $\text{Tb}(\text{X}_4\text{TPP})(\text{OAc})$  complexes are more readily reduced and oxidized relative to the corresponding free bases, **5** and **7**. However, concerning the metalated derivatives of the octahalogenated species (**10** and **12**), these are slightly easier to oxidize but considerably less easy to reduce, than their free base precursors. This, as expected, results in a larger HOMO–LUMO gap for the  $\text{Tb}(\text{X}_8\text{TPP})(\text{OAc})$  complexes relative to their free bases, **6** and **8**. However, regarding the Soret transition energies of  $\text{Tb}(\text{X}_4\text{TPP})(\text{OAc})$  and  $\text{Tb}(\text{X}_8\text{TPP})(\text{OAc})$ , they are clearly red-shifted relative to those of the free base analogues, as previously stated, in contrast to predicted values.<sup>18,23,24</sup> Interestingly,  $\text{Tb}(\text{X}_8\text{TPP})(\text{OAc})$  **10** and **12** are somewhat less easily oxidized than the corresponding  $\text{Tb}(\text{X}_4\text{TPP})(\text{OAc})$  species, **9** and **11**, despite their higher number of halogen substituents, unlike the case of iron  $\beta$ -octabromoporphyrins.<sup>26,86</sup> However, these results suggest that the bulky, electron-rich Tb ion either decreases the degree of distortion of the porphyrin macrocycle or the contribution of the metallic orbitals modulates the energies of the redox-active orbitals of the ring.

**Description of the Structures.** An ORTEP diagram of  $\text{Ni}(\text{Cl}_8\text{TPP})$  with an atomic labeling scheme is given in Figure 2, and selected bond distances and angles are listed in Table 4. The coordination geometry around Ni is square tetragonal with bond lengths ranging from 1.899(6) to 1.911(6) Å (mean value  $\text{Ni}-\text{N} = 1.909$  Å). The metal lies on the mean plane of the  $\text{C}_{20}\text{N}_4$  core atoms (mean deviation 0.005 Å). The presence of nickel in the macrocyclic cavity along with the substitution on the  $\text{C}_\beta$  and  $\text{C}_m$  atoms of the porphyrin results in the saddle and ruffling of the ligand. The mean absolute displacement of the nitrogen atoms from the  $\text{C}_{20}\text{N}_4$  mean plane is 0.14 Å. In the more substituted porphyrinic Ni complexes<sup>19</sup>  $\text{H}_2(\text{Br}_8\text{TMP})$  (2,3,7,8,12,13,17,18-octabromo-5,10,15,20-tetramesitylporphyrin) and  $\text{H}_2(\text{Br}_8\text{Tp-FPP})$  [2,3,7,8,12,13,17,18-octabromo-5,10,15,20-tetrakis(pentafluorophenyl)porphyrin], the deviation of the four nitrogen atoms from the  $\text{C}_{20}\text{N}_4$  mean plane is 0.19 and 0.20 Å, respectively. The presence of the chlorine atoms in  $\text{C}_\beta$  carbon atoms of the porphyrin skeleton in  $\text{Ni}(\text{Cl}_8\text{TPP})$  results in the

(85) Barkigia, K. M.; Renner, M. W.; Furenlid, L. R.; Medforth, C. J.; Smith, K. M.; Fajer, J. *J. Am. Chem. Soc.* **1993**, *115*, 3627.

(86) Kadish, K.; Autret, M.; Ou, Z.; Tagliatesta, P.; Boschi, T.; Fares, V. *Inorg. Chem.* **1997**, *36*, 204.

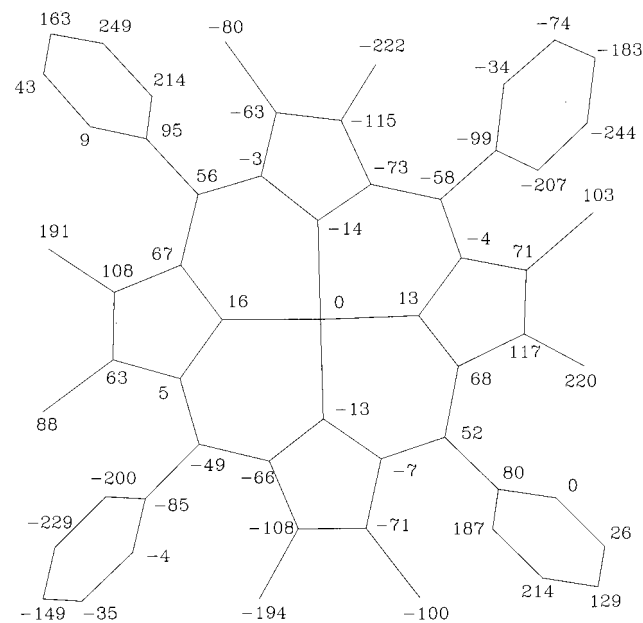
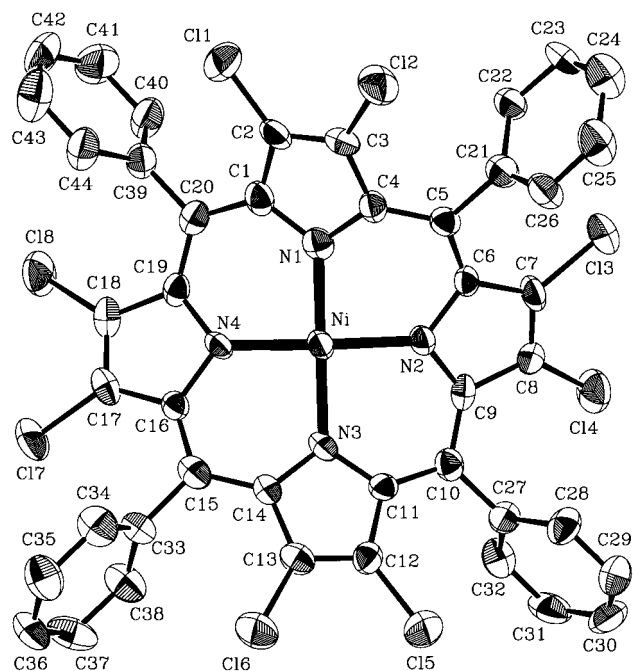


**Figure 2.** ORTEP diagram of Ni(Cl<sub>8</sub>TPP) with 50% thermal probability ellipsoids showing the atomic labeling scheme with the corresponding figure showing the displacement of core atoms from the mean plane.

saddling distortion of the ligand, expressed by the mean absolute displacement of the C<sub>β</sub> atoms from the C<sub>20</sub>N<sub>4</sub> mean plane (0.67 Å for C<sub>2</sub>, C<sub>7</sub>, C<sub>12</sub>, C<sub>17</sub> and 1.12 Å for C<sub>3</sub>, C<sub>8</sub>, C<sub>13</sub>, C<sub>18</sub>). The average absolute displacement of the corresponding chlorine atoms bonded to C<sub>β</sub> atoms is 0.93 (for Cl<sub>1</sub>, Cl<sub>3</sub>, Cl<sub>5</sub>, Cl<sub>7</sub>) and 2.07 Å (for Cl<sub>2</sub>, Cl<sub>4</sub>, Cl<sub>6</sub>, Cl<sub>8</sub>). A comparison of these values with those reported for Ni(Br<sub>8</sub>TMP) and Ni(Br<sub>8</sub>TpFPP) (Table 5) indicates that Ni(Cl<sub>8</sub>TPP) is somehow less saddle distorted. The C<sub>β</sub> and Br displacements from the C<sub>20</sub>N<sub>4</sub> mean plane for Ni(Br<sub>8</sub>TMP) are 1.20/0.80 and 2.16/1.26 Å, respectively, and for Ni(Br<sub>8</sub>TpFPP), these values are 1.24/1.08 and 2.23/1.84 Å, respectively. The presence of the metal ion in the porphyrin cavity in

**Table 4.** Selected Bond Distances (Å), Angles (deg), and Averages for Ni(Cl<sub>8</sub>TPP) H<sub>2</sub>(Br<sub>8</sub>TPP)·2DMF and Tb(Cl<sub>8</sub>TPP)(OAc)(DMSO)<sub>2</sub>·3PhCH<sub>3</sub>·MeOH

bonds	Ni(Cl <sub>8</sub> TPP)	H <sub>2</sub> (Br <sub>8</sub> TPP)·2DMF	Tb(Cl <sub>8</sub> TPP)(OAc)
M–N(1)		1.911(6)	2.41(1)
M–N(2)		1.899(6)	2.431(9)
M–N(3)		1.908(6)	2.44(1)
M–N(4)		1.900(6)	2.43(1)
N–C <sub>a</sub>	1.384	1.361	1.381
C <sub>a</sub> –C <sub>b</sub>	1.443	1.434	1.444
C <sub>b</sub> –C <sub>b</sub>	1.348	1.348	1.358
X–C <sub>b</sub>	1.705	1.879	1.72
C <sub>a</sub> –C <sub>m</sub>	1.394	1.418	1.404
C <sub>m</sub> –C <sub>phenyl</sub>	1.488	1.481	1.505
(N–M–N) <sub>cis</sub>	90.3		73.8
(N–M–N) <sub>trans</sub>	171.6		116.2
C <sub>a</sub> –N–C <sub>a</sub>	107.3	109.3	107.4
N–C–C <sub>b</sub>	108.3	107.5	108.4
C <sub>a</sub> –C <sub>b</sub> –C <sub>b</sub>	107.7	107.7	107.6
N–C <sub>a</sub> –C <sub>m</sub>	123.9	123.5	124

**Table 5.** Structural Characteristics between Ni Perchlorinated and Ni Perbrominated Porphyrins, Indicating the Distortion of Porphyrin Core

atom(s)	Average Displacement of Selected Atoms of Porphyrin from C <sub>20</sub> N <sub>4</sub> Mean Plane		
	Ni(Cl <sub>8</sub> TPP)	Ni(Br <sub>8</sub> TPP)	Ni(Br <sub>8</sub> TpFPP)
N	0.14	0.19	0.20
C <sub>m</sub>	0.54	0.36	0.18
C <sub>β</sub>	0.67 <sup>a</sup> , 1.12 <sup>b</sup>	1.20, 0.80 <sup>c</sup>	1.24 <sup>a</sup> , 1.08 <sup>b</sup>
Cl <sub>1</sub> /Br <sub>1</sub>	0.93	2.16	2.23
Cl <sub>2</sub> /Br <sub>2</sub>	2.07	1.26	1.84
group	Dihedral Angles with the C <sub>20</sub> N <sub>4</sub> Mean Plane		
	Ni(Cl <sub>8</sub> TPP)	Ni(Br <sub>8</sub> TPP)	Ni(Br <sub>8</sub> TpFPP)
pyrroles	34.0, 32.9	36.00	36.40, 41.40
	28.3, 27.1		
phenyls	52.2, 54.3	58.30	39.80, 45.70
	59.4, 63.0		47.00, 48.10

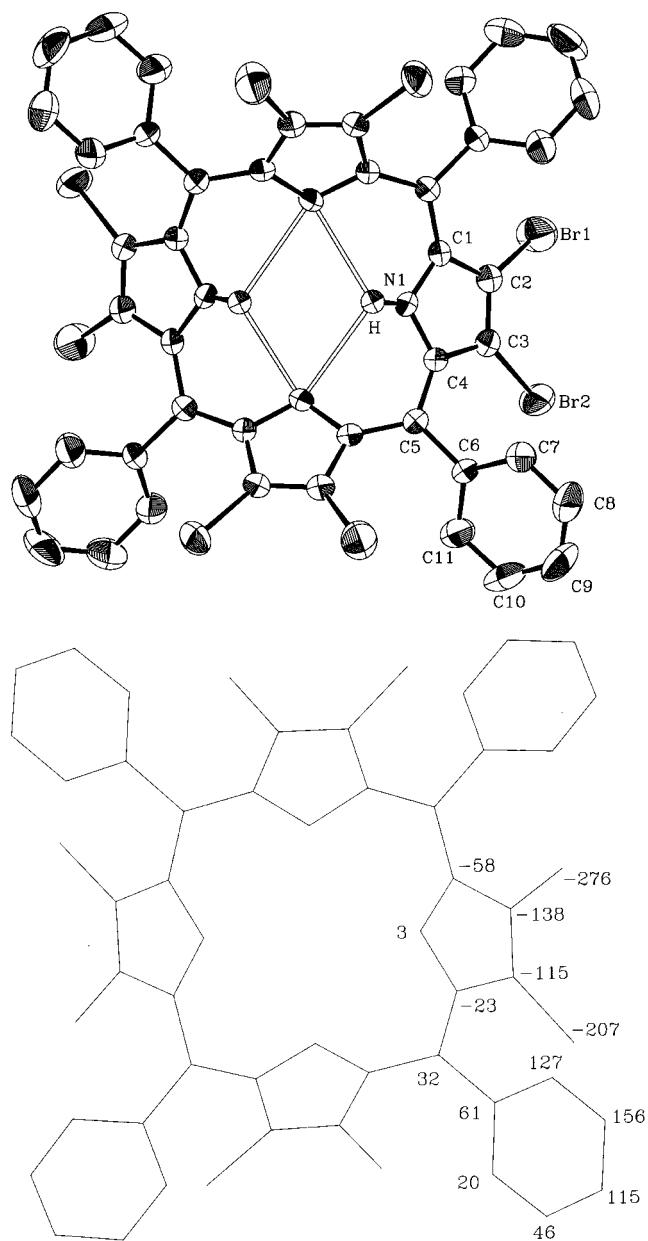
<sup>a</sup> Average value of C<sub>2</sub>, C<sub>7</sub>, C<sub>12</sub>, C<sub>17</sub> displacements. <sup>b</sup> Average value of C<sub>3</sub>, C<sub>8</sub>, C<sub>13</sub>, C<sub>18</sub> displacements. <sup>c</sup> Average value of C<sub>2</sub>, C<sub>3</sub> displacements.

combination with the phenyl substituents on the C<sub>m</sub> atoms result in the twist distortion of the molecule. The average deviation of the C<sub>m</sub> atoms from the C<sub>20</sub>N<sub>4</sub> mean plane is 0.54 Å, which is larger than the values of 0.36 and 0.18 Å reported for Ni(Br<sub>8</sub>TMP) and Ni(Br<sub>8</sub>TpFPP), respectively. The short nickel–nitrogen bond length (mean 1.904 Å) is also responsible for the twist distortion observed in the porphyrin skeleton. Because of the larger steric effects observed in the phenyl substituted bromoporphyrins in Ni(Br<sub>8</sub>TMP) and Ni(Br<sub>8</sub>TpFPP), the phenyl rings rotate toward the mean porphyrin plane by angles of 58.3(6)° and 39.8(6)°–48.1(5)°, respectively. In the case of Ni(Cl<sub>8</sub>TPP), the steric effects between the chlorine substituents and the phenyl rings are not so severe, and the phenyl rings are less rotated with respect to the C<sub>20</sub>N<sub>4</sub> mean plane (52.2°, 54.3°, 59.4°, and 63.0°). The substituted pyrrole rings are coplanar within experimental error. The slightly increased distortion caused by the nickel insertion is reflected in the different displacements of the chlorine atoms from the mean pyrrole plane (mean values: 0.05 Å for Cl<sub>1</sub>, Cl<sub>3</sub>, Cl<sub>5</sub>, Cl<sub>7</sub> and 0.23 Å for Cl<sub>2</sub>, Cl<sub>4</sub>, Cl<sub>6</sub>, Cl<sub>8</sub>). In the case of Ni(Br<sub>8</sub>TMP) and Ni(Br<sub>8</sub>TpFPP), these values are 0.09 (Br<sub>1</sub>), 0.24 (Br<sub>2</sub>) and 0.15 (Br<sub>1</sub>), 0.27 Å (Br<sub>2</sub>), respectively. The substituted pyrrole rings are tilted alternatively up and down with respect to the

**Table 6.** Intra- and Intermolecular H-bonds Observed in the X-ray Crystal Structure of  $\text{H}_2(\text{Br}_8\text{TPP})$ 

Intramolecular		
N—H $\cdots$ N	N $\cdots$ N	N—H $\cdots$ N (angle ( $^\circ$ ))
2.510(6)	2.955(6)	113.3(4)
(0.25 + y, 0.75 - x, -0.25 - z)		
2.617(6)	2.955(6)	104.7(4)
(0.25 + y, 0.75 - x, -0.25 - z)		
Intermolecular		
N—H $\cdots$ O	N $\cdots$ O	N—H $\cdots$ O (angle ( $^\circ$ ))
2.18(1)	3.01(1)	162.6(6)
(0.25 + y, 0.75 - x, -0.25 - z)		

porphyrin—core mean plane by  $34.0^\circ$ ,  $32.9^\circ$ ,  $28.3^\circ$ , and  $27.1^\circ$ , while in  $\text{Ni}(\text{Br}_8\text{TMP})$  the tilting is  $36.0(5)^\circ$ , and in  $\text{Ni}(\text{Br}_8\text{TpFPP})$ , it ranges from  $36.4(8)^\circ$  to  $41.4(8)^\circ$ . The compound  $\text{H}_2(\text{Br}_8\text{TPP})$  crystallizes in the tetragonal space group  $I4_1/a$ ; the origin was taken on the center of symmetry. The asymmetric unit contains one quadrant of the  $\text{H}_2(\text{Br}_8\text{TPP})$  molecule and one-half of a DMF solvent molecule. The oxygen and the nitrogen atoms of the DMF sit on a  $C_2$  axis; therefore, the molecule is disordered. The structure consists of chains directed parallel to the  $c$ -axis formed by alternating porphyrin molecules and two DMF solvent molecules. An ORTEP diagram of the molecule with the atomic labeling is given in Figure 3, selected bond distances and angles are presented in Table 4, while H-bonds are given in Table 6. Two types of H-bonds are observed: (i) bifurcated H-bonds inside the porphyrin core, also observed in other porphyrin derivatives,<sup>87</sup> and (ii) intermolecular H-bonds between the N—H group and the oxygen atom of the DMF solvent molecule. An ORTEP diagram of  $\text{Tb}(\text{Cl}_8\text{TPP})(\text{OAc})(\text{DMSO})_2 \cdot 3\text{PhCH}_3 \cdot \text{MeOH}$  with the atomic labeling scheme is given in Figure 4, and selected bond distances are given in Table 4. A detailed description of the structures of  $\text{H}_2(\text{Br}_8\text{TPP}) \cdot 2\text{DMF}$  and  $\text{Tb}(\text{Cl}_8\text{TPP})(\text{OAc})(\text{DMSO})_2 \cdot 3\text{PhCH}_3 \cdot \text{MeOH}$  has been given elsewhere.<sup>29</sup> A comparison of the structural characteristics of the three structures reported herein is given in Tables 6 and 7. Considering the octachloro complexes of Ni and Tb, great differences in the distortion of the porphyrin are observed. The insertion of the relatively small nickel ion into the cavity of the macrocycle results in its twisted distortion expressed by the  $C_m$  displacement from the  $C_{20}\text{N}_4$  mean plane ( $0.54 \text{ \AA}$ ). On the contrary, the relatively larger terbium ion lies  $1.42 \text{ \AA}$  out of the  $C_{20}\text{N}_4$  mean plane; thus, no twisted distortion is observed ( $C_m$  displacement =  $0.025 \text{ \AA}$ ). The saddle distortion, expressed by the  $C_\beta$  displacement from the  $C_{20}\text{N}_4$  mean plane, dominates in both structures. As has been observed in a series of porphyrins and their metal derivatives,<sup>88,89</sup> there is a strong tendency that as the  $C_\beta$  displacement increases the phenyl rings become much more nearly coplanar with the porphine nucleus because of the extreme tilting of the pyrrole rings. These trends are also

**Figure 3.** ORTEP diagram of  $\text{H}_2(\text{Br}_8\text{TPP})$  with 50% thermal probability ellipsoids showing the atomic labeling scheme with the corresponding figure showing the displacement of core atoms from the mean plane.

observed in our complexes. In the case of the free base  $\text{H}_2(\text{Br}_8\text{TPP})$ , the saddle distortion ( $C_\beta = 1.382/1.145 \text{ \AA}$ ) and the tipping of the pyrrole rings ( $44.4^\circ$ ) results in particularly acute dihedral angles for the phenyl rings relative to the  $C_{20}\text{N}_4$  mean plane ( $29.7^\circ$ ).

### Concluding Remarks

For all the compounds studied, the presence of eight halogens on the porphyrin  $\beta$ -pyrrole positions caused a larger red shift of the Soret band than the presence of four halogens. As expected, brominated derivatives present the larger shift for the Soret band. Bromine is slightly less electronegative than chlorine but causes larger distortions on the porphyrin, and spectral red-shift has been found to be strongly coupled to the degree of ring distortion.<sup>22</sup> However, the absolute value

(87) Chan, K. S.; Zhou, X.; Luo, B. S.; Mak, T. C. W. *J. Chem. Soc., Chem. Commun.* **1994**, 271.

(88) Silvers, S. J.; Tulinsky, A. *J. Am. Chem. Soc.* **1967**, 89, 3331.

(89) Scheidt, W. R.; Lee, Y. J. In *Metal Complexes with Tetrapyrrole Ligands I*; Buchler, J. W., Ed.; Springer-Verlag: New York, 1987; p 2.

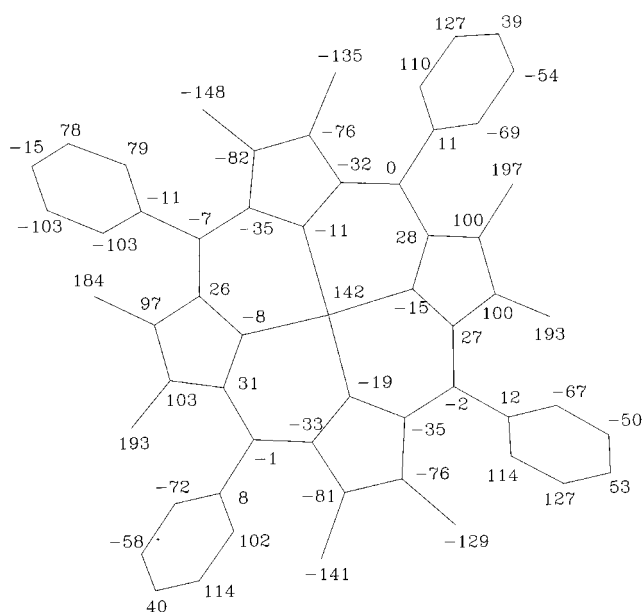
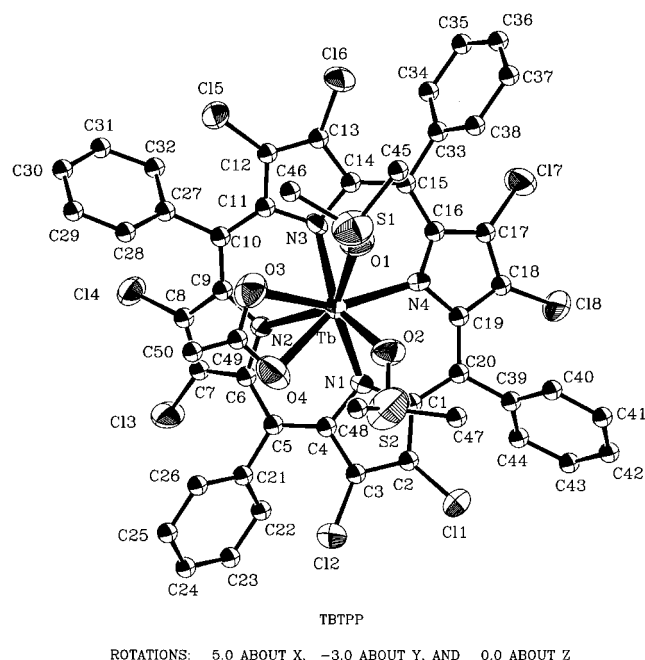


**Figure 4.** ORTEP diagram of  $\text{Tb}(\text{Cl}_8\text{TPP})(\text{OAc})(\text{DMSO})_2 \cdot 3\text{PhCH}_3 \cdot \text{MeOH}$  with 50% thermal probability ellipsoids showing the atomic labeling scheme with the corresponding figure showing the displacement of core atoms from the mean plane.

of  $\lambda_{\text{max}}$  is not the same for free porphyrin and its metalated complexes. So, absorption bands in the electronic spectra of the free bases are more shifted to the red than those of the Ni complexes. The absorption bands of the terbium complexes are the most red shifted in the series of the compounds studied. The absolute value,  $\lambda_{\text{max}}$ , of the Soret band in the case of octahalogenated compounds follows the order Tb complexes > free bases > Ni complexes. The same holds for tetrahalogenated derivatives, though differences are less pronounced. Although in the case of halogen-induced free-porphyrin distortion the most deformed ring exhibits the most red-shifted Soret absorption band (in case of  $\text{Br}_8\text{TPP}$  derivatives), this is not the case for the metal-induced distortion

**Table 7.** Structural Characteristics of  $\text{H}_2(\text{Br}_8\text{TPP}) \cdot 2\text{DMF}$  and  $\text{Tb}(\text{Cl}_8\text{TPP})(\text{OAc})(\text{DMSO})_2 \cdot 3\text{PhCH}_3 \cdot \text{MeOH}$ , Indicating the Distortion of Porphyrin Core

Average Displacement ( $\text{\AA}$ ) of Selected Atoms of Porphyrin from $\text{C}_{20}\text{N}_4$ Mean Plane		
atom(s)	$\text{Tb}(\text{Cl}_8\text{TPP})(\text{OAc})$	$\text{H}_2(\text{Br}_8\text{TPP})^a$
N	0.134	0.033
$\text{C}_m$	0.025	0.317
$\text{C}_b$	0.90, 0.88 <sup>a</sup>	1.382, 1.145 <sup>b</sup>
$\text{Cl}_1/\text{Br}_1$	1.67 <sup>c</sup>	2.764 <sup>e</sup>
$\text{Cl}_2/\text{Br}_2$	1.63 <sup>d</sup>	2.069 <sup>e</sup>
Dihedral Angles with the $\text{C}_{20}\text{N}_4$ Mean Plane		
group	$\text{Tb}(\text{Cl}_8\text{TPP})(\text{OAc})$	$\text{H}_2(\text{Br}_8\text{TPP})$
pyrrolys	19.6, 33.4	44.4
	21.7, 35.5	
phenyls	47.6, 49.6	29.7
	50.9, 49.6	

<sup>a</sup> Average value of  $\text{C}_2$ ,  $\text{C}_7$ ,  $\text{C}_{12}$ ,  $\text{C}_{17}$  and  $\text{C}_3$ ,  $\text{C}_8$ ,  $\text{C}_{13}$ ,  $\text{C}_{18}$  displacements, respectively. <sup>b</sup> Average value of  $\text{C}_2$ ,  $\text{C}_3$  (and their symmetrical atoms) displacements. <sup>c</sup> Average value of  $\text{Cl}_1$ ,  $\text{Cl}_3$ ,  $\text{Cl}_5$ ,  $\text{Cl}_7$  displacements. <sup>d</sup> Average value of  $\text{Cl}_2$ ,  $\text{Cl}_4$ ,  $\text{Cl}_6$ ,  $\text{Cl}_8$  displacements. <sup>e</sup> Average value of  $\text{Br}_1$  (and its symmetrical atoms) and  $\text{Br}_2$  (and its symmetrical atoms) displacements.

of  $\text{Cl}_8\text{TPP}$  complexes. The half-wave potentials measured for all the free porphyrins are in good agreement with the potentials measured for the tetra- and octahalogenated derivatives of 5,10,15,20-tetramesitylporphyrins.<sup>75</sup> All the Tb complexes oxidized easier than the corresponding free bases, while only Tb tetrahalogenated complexes reduced easier with respect to their free bases. The HOMO–LUMO energy gap for all the halogenated compounds studied varies from 2.22 to 1.70 V and is smaller than that of the free TPP which measured 2.32 V.<sup>75</sup> The HOMO–LUMO gap is found to be considerably smaller in the case of tetrahalogenated Tb complexes than the corresponding free bases, while for octahalogenated Tb complexes it is somewhat larger when compared with the corresponding free porphyrins. The possibility that electron-transfer processes involve molecular orbitals with major or minor metal character could not be excluded, and studies on the whole series of lanthanide perhalogenated complexes are under way.<sup>90</sup> However, systematic studies of mono- or bisporphyrinates along the series of lanthanide ions demonstrate that the electrode reactions observed are porphyrin-centered. Because the crystal structures of the Ni and Tb complexes with the octachlorinated porphyrin are available, a structure–properties correlation could be attempted. Tb complexes exhibit Soret transitions of lower energy than Ni complexes, and the effect is particularly pronounced in the case of octahalogenated compounds. In this case, the Soret absorption band was found more than 20 nm bathochromically shifted for Tb complexes, with respect to those of Ni. However, if the energy of electronic transitions is governed by the distortion of the porphyrin (either because of the peripheral substituents or because of the metal ion), then the compound with the more distorted macrocycle should exhibit the lowest energy Soret band. According to the data acquired during the X-ray diffraction studies of the Tb and Ni compounds, the more

(90) Spyroulias, G. A.; Coutsoulelos, A. G. Work in progress.

distorted porphyrin is found to be Ni(Cl<sub>8</sub>TPP), manifested by the C<sub>m</sub> displacement. Consequently, the metal derivative of the octachlorinated TPP with the most distorted ring exhibits the higher Soret transition energy, and we can deduce that the nature of the metal ion could strongly influence the properties of the complexes in addition to the already mentioned reasons. The X-ray data obtained indicate that in the series of metal complexes of (Cl<sub>8</sub>TPP)<sup>2-</sup> the size of the metal ion compensates to the ring distortion. The most distorted porphyrin ring manifested by the displacements of pyrrole nitrogens and C<sub>m</sub> from planarity is found for the complex with the smaller metal ion, the Ni. The terbium ion lies 1.28 Å out of the N<sub>4</sub> mean plane, while the Ni, with considerably smaller ionic radius, is hosted in the macrocycle cavity causing core contraction.<sup>19</sup> However, the crystal structure of the free H<sub>2</sub>(Cl<sub>8</sub>TPP) is not available, and thus, the different effect of each metal ion could not be safely concluded. One should mention that when free porphyrin and the Ni complex of octabromo derivatives of tetramesitylporphyrin and tetra(pentafluorophenyl)porphyrin are compared, the distortion of the Ni complex is found to be more

severe (on the basis of UV–vis data). The effect of metal size on the distortion and consequently on the properties of partially halogenated or perhalogenated porphyrin derivatives is of particular interest. Studies including the rational synthesis of new perhalogenated metalloporphyrins or metal-free porphyrins in order to monitor the conformational and physicochemical changes of those compounds are currently in progress.<sup>90</sup>

**Acknowledgment.** This research was supported by the Greek General Secretariat of Research and Technology, the Centre National de la Recherche Scientifique, and the Paul Sabatier University of Toulouse and Elais corporation. We are also grateful to Mr. John Boutaris and the Agricultural Bank of Greece (A.T.E.) for financial support to C.P.R. as well as the two reviewers for their insightful comments.

**Supporting Information Available:** Detailed experimental data for X-ray structural analyses. This material is available free of charge via the Internet at <http://pubs.acs.org>.

IC000738H